Microaneurysms Segmentation in Retinal Images for Early Detection of Diabetic Retinopathy

N.Mazlan, H.Yazid, S. A. Rahim and S.N Basah
School of Mechatronics, University Malaysia Perlis, 02600, Arau, Perlis, Malaysia
atikahmazlan250692@gmail.com

***Abstract*—Microaneurysms (MAs) are the tiny aneurysms which show the earliest sign of diabetic retinopathy (DR). MAs might progress and harm human eyes if not treated. This paper presents an automatic method for segmentation of MAs in order to control the progression of DR. MESSIDOR database of 40 random images were utilised for further processing. The proposed approach covered pre-processing steps, contrast enhancement, filtration and segmentation by h-maxima transform and multilevel thresholding. Some post-processing techniques also involved in this approach using morphological operation. The detected MAs determined the grade of disease severity. The result showed that the percentage of severity disease detected was 60%.**

***Index Terms*—Diabetic Retinopathy; H-maxima Transform; Multilevel Thresholding; Morphological Closing; Microaneurysms Segmentation.**

I. INTRODUCTION

Currently, the main challenge of health care issues is the progression of diabetes mellitus (DM). DM is widely spread through all people over the world and cause vascular changes in the human body. In the next 25 years, World Health Organisation (WHO) expects that the people who afflicted from diabetes will rise from130 million to 350 million [1]. This illness will result in a renal problem, heart disease and retinopathy [2]. The common problem of diabetes is diabetic retinopathy. DR occurs at the back of the retina and develops the small changes of the vascular pattern. As the disease progress, it will cause visual impairment such as blurred vision and blindness.

DR can be widely classified as non- proliferative diabetic retinopathy (NPDR) and proliferative diabetic retinopathy (PDR). For easy understanding, NPDR refers to the earliest symptom of diabetic retinopathy that develops lesions such as microaneurysm (MAs), haemorrhages (HMAs), soft exudates, and venous bending [3]. NPDR was graded into four main stages namely normal, mild NPDR, moderate NPDR and severe NPDR [4]. In contrast, PDR is the advanced stage of the illness. New abnormal blood vessel (neovascularization) is grown inside the surface of the retina due to lacking oxygen [5]. The retinal blood vessel becomes fragile and ruptured, thus leads to permanent vision loss [4].

Recently, this issue has captured the researcher's attention all over the world. The growth of diabetic retinopathy can be control through automatic detection of MAs. MAs is the first clinical sign of DR [6]. However, the detection process will become quite complicated since the size of MA is very tiny, hard to be detected by naked eye. MAs appear red, similar to retinal vessels and haemorrhages. The location of MA near to the weak intensity vessels also develops some challenge for detection of MAs.

In 2016 [6], Raghu M.U et al. proposed a simpler approach using morphological transform to detect MAs. The detection of MAs was done through the removal of retinal vessels and other undesired lesions. This approach was supported by Nemade et al. [7]. Sopharak et al. [8] detected the MAs by using a set of optimally adjusted morphological operators. This method was quite challenging since it was tested on the non-dilated pupil and low contrast retinal images. In 2013 [4], Sopharak et al. improved the study from the previous research [8] by using a simple hybrid morphological based method. To increase the efficiency of the result, Naive Bayes classifier was applied in the segmentation stage.

Previously, Marwan et al. used h-maxima and multilevel thresholding method to detect retinal vessels [9]. In 2013, S.SB et al. [10] described similar method recently published by Marwan et al. [11]. They used multi-level thresholding segmentation for the detection of MAs in digital eye fundus image. In this research, the earliest symptoms of diabetic retinopathy were detected. In comparison with [9], Marwan et al. have detected retinal vessels only without the detection of MAs. Thus, this research was improvised up to the detection of MAs and its severity grade.

The goals of this research are to detect MAs and determine the severity grade of the images compared to ground truth. The flow of MAs segmentation is structured as follows. Section 2 deals with methodologies and proposed algorithm for MAs detection. Section 3 demonstrates the result and discussion. Finally, section 4 draws some related conclusion.

II. PROPOSED METHODOLOGY

A. Dataset

This research presented a pixel-based method for MAs segmentation using MESSIDOR database. MESSIDOR database contained 1200 eye colour fundus images formatted in TIFF file, diagnosed by three ophthalmologic departments. The images were packed in three sets in which one ophthalmologic department was assigned for one dataset. Each set is divided into four zipped subset file containing 100 images per subset. The retinal images were captured with an eight bits per colour plane and a 45-degree field of view by a video colour 3CCD camera on a Topcon TRC NW6 non-mydriaticretinograph[12]. Three different pixel matrix sizes of 1440 × 960, 2240 × 1488 and 2304 × 1536 were utilised in this database [13]. The ground truth retinopathy grading diagnosed by the expertise also presented in this database for comparison with detected MAs. 40 random images over 1200 were selected for the testing purpose. MESSIDOR database contained various lesions such as exudates, haemorrhages and MAs. In this study, only 40 images with the presence of MAs were chosen. The flowchart of this approach is illustrated in Figure 1.

B. Pre-processing

1) RGB to Green Channel Conversion

MESSIDOR dataset consists of colour fundus image from three main colour information namely red channel (R), green channel (G) and blue channel (B). Each colour information contained intensity from 0 (dark) to 255 (white). In this study, the normalised green channel was extracted for further processing since it exhibits better contrast and less noise compared to red and blue channel [10]. The mathematical equation for green channel is stated in Equation (1).

$$g = \frac{G}{R + G + B} \tag{1}$$

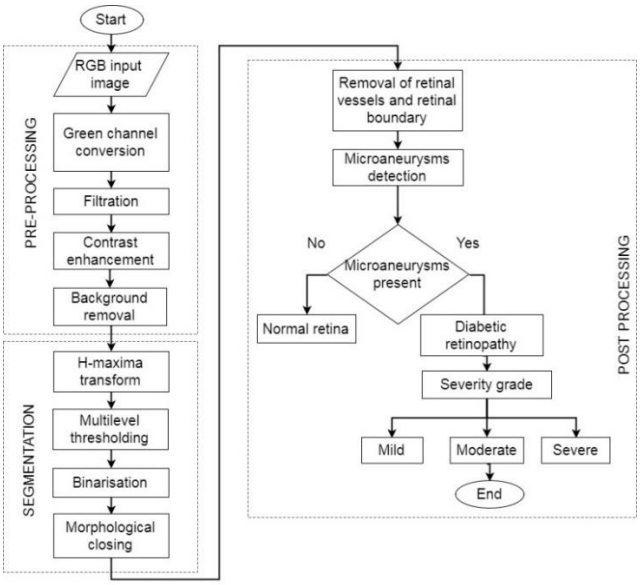

Figure 1: Flowchart of the proposed methodology

The green channel denotes by g whereas R, G, and B refer to red, green and blue colour information. Figure 2 demonstrates the RGB image and green channel image.

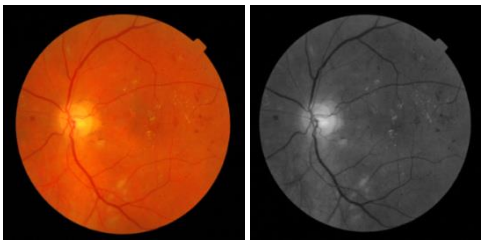

(a) (b)

Figure 2 : (a) RGB image (b) Green channel image

2) Filtration - Min Filter

The min filter helps to enhance the dark object in the image by increasing its intensity value. The retinal vessels and dark lesion have dark colour information. Thus, the implementation of min filter helps to highlight and visualised retinal vessels and dark lesions more clearly. In this approach, the windowing size 3×3 was used since it produced a better quality of the image and as presented in Figure 3.

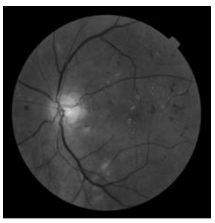

Figure 3: Min filter image

3) Contrast Enhancement

Contrast enhancement was implemented by using morphological top and bottom hat transformation method to improve the contrast of input images as shown in Figure 4.

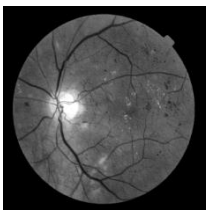

Figure 4: Enhancement by morphological top and bottom hat

Morphological top and bottom hat transform is the combination of top hat transformation and bottom hat transformation of morphological operation. This technique improves the contrast and highlight details of foreground better than contrast limited adaptive equalisation (CLAHE). In addition, the limited noise was produced and able to be controlled by applying Wiener filtering. The mathematical formula for top hat transformation, bottom hat transformation and enhancement by top and bottom hat transformation are described in Equation (2), Equation (3) and Equation (4).

$$T_{hat}(g) = g - (g \circ SE) \tag{2}$$

$$B_{hat}(g) = (g \bullet SE) - g \tag{3}$$

$$E_{TB}(g) = \big(g + T_{hat}(g)\big) - B_{hat}(g) \tag{4}$$

where, $T_{hat}(g)$ presents top hat transformation, $B_{hat}(g)$ refers to bottom hat transformation, $E_{TB}(g)$ demonstrates enhancement by top and bottom transformation, SE is a structuring element, $(g \circ SE)$ and $(g \bullet SE)$ represents morphological opening and closing of min filter, g and structuring element .

4) Background Exclusion

This approach aims to remove background variation illumination problem so that the foreground objects will be visualised easily. Median filtering, f_{med} of windowing size 36×36 was used for smoothing effect. Based on Equation (5), the background exclusion was obtained by subtracting the enhanced top and bottom morphological transformation image, E_{TB} from median filtered image, f_{med}

$$\hat{f} = f_{med} - E_{TB} \tag{5}$$

Median filtering was capable of removing the background and maintaining the sharp edges of the retinal boundary [9]. Removal of background leads to highlight the vessels and MAs. The resulting image is shown in Figure 5.

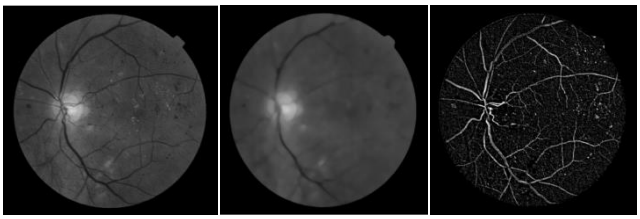

(a) (b) (c)

Figure 5: (a) Contrast-enhanced image, E_{TB} (b) Median smoothing image, f_{med} (c) Background exclusion image, $\hat{f}$

5) Wiener Filter

After background exclusion steps, the contrast of the obtained images was improved. However, it develops blurriness and some additive white noise (salt). Hence, this wiener filter helps to eliminate the blurriness and additive noise in the image [14]. The Wiener filter can be calculated using Equation (6).

$$W(u,v) = \frac{H^*(u,v)P_S(u,v)}{|H(u,v)|^2 + P_n(u,v)/P_S(u,v)} \quad (6)$$

$H(u,v)$ is a degradation function, $H^*(u,v)$refers to complex conjugate of degradation function $H(u,v)$, $P_n(u,v)$ denotes by power spectral of noise and $P_s(u,v)$ is power spectral un-degraded image. In fact, wiener filter is a linear filter which help to blur the image and at the same time maintaining the sharpness of the image as shown in Figure 6.

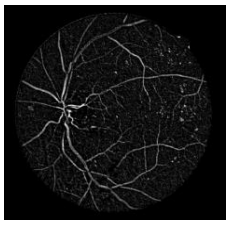

Figure 6: Weiner filtering image

C. Segmentation of Microaneurysms

1) H-maxima Transform

H-maxima transform was implemented to reduce the number of the intensity level of the pre-processed image. The h-maxima transform, H_t was used to suppress all maxima in the intensity image, i whose height is less than the threshold value, t. Equation (7) describes the mathematical equation for h-maxima transforms.

$$H_t(i) = R_i^{\delta}(i - t) \quad (7)$$

i expresses an intensity value, H indicates h-maxima transform, t refers to a threshold value and R_i^{δ} represents morphological reconstruction by dilation. Figure 7 illustrates the resulting image for h-maxima transforms.

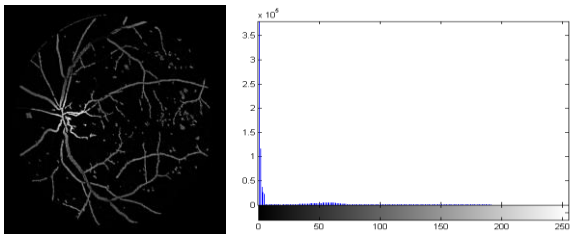

Figure 7: H-maxima image and its histogram distribution

2) Multilevel thresholding

Multilevel thresholding is one type of thresholding techniques which plays a vital role in image segmentation [15]. In this stage, h-maxima image that contained grey level information was converted to an indexed image. The image was partitioned into several distinct regions depending on its threshold value. The threshold value, Ti can be selected by analysing the histogram pattern of the image as shown in Figure 8. More than one threshold value was needed to apply this technique [9-10]. This technique aims to partition the pixels of intensity image into N groups, $G_1 \ldots . G_N$ based on needed threshold values, T_i [9]. The multilevel thresholding formula is illustrated in Equation (8).

$$T_i = \frac{i}{N-1}, \frac{i+1}{N-1}, \ldots, \frac{N-2}{N-1}, \quad i = 1, \ldots, N-1 \quad (8)$$

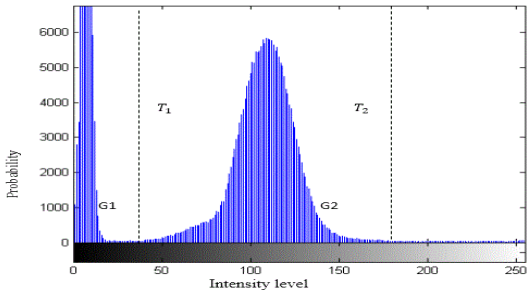

Figure 8: The partitioned of regional group G_1 and G_2 is based on threshold T_1, T_2 respectively.

In this study, four threshold values with three regional maxima were implemented. The regional maxima were classified into the background and several foregrounds such as retinal vessels, MAs and haemorrhages. This technique minimised the complexity of segmented image since less intensity value need to be analysed [16]. Figure 9 illustrates the resulting image of multilevel thresholding technique and its histogram distribution.

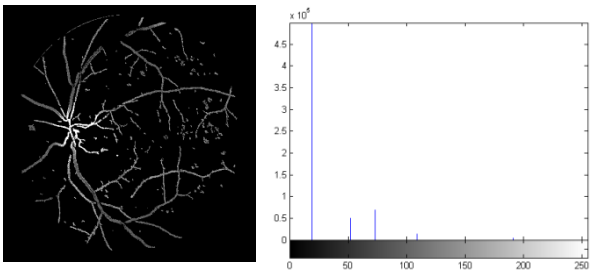

Figure 9: Indexed image and histogram distribution of four threshold value

3) Binarisation

Binarisation is the process of converting a grayscale image into a binary image through thresholding. Thresholding

separates the image into background and foreground containing two intensity values which are white (1) and black (0). Reducing in intensity level will result in reducing storage space and improving processing speed. In this approach, the intensity level, I_T greater than the minimum threshold value, T_{min} was set as foreground (1) and else will act as background (0). Equation 9 demonstrates the mathematical equation of the applied technique. The binary image, BW_1 is obtained through thresholding technique as shown in Figure 10.

$$BW_1(x,y) = \begin{cases} 1 & if\ I_T(x,y) > T_{min} \\ 0 & otherwise \end{cases} \quad (9)$$

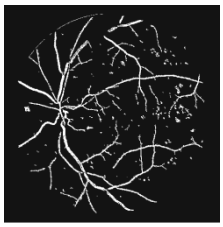

Figure 10: Binary image, BW1

4) Morphological Closing

The fundamental of morphological close operation is a dilation followed by erosion. Dilation was used to grow the object in an image while erosion shrinks the object image [17]. The result of dilation and erosion was influenced by the size and shape of structuring element. The closing of image f by structuring element s, denotes by $f \bullet s$ is a dilation, $\oplus$ followed by an erosion, $\ominus$ .The morphological closing equation is demonstrated in Equation (10).

$$f \cdot s = (f \oplus s) \ominus s \quad (10)$$

The specialities of morphological closing are it able to fill the hole between the region and keeping the initial region size. Some gap that has been detected between the foregrounds should be filled to connect all desired components. These issues were solved by utilising morphological close operation.

D. Post Processing

1) Removal of Retinal Boundary

As a result of thresholding technique, some undesired pixels like retinal frame were detected. To refine and maintain the accuracy of microaneurysm detection, this frame should be eliminated. The subtraction of the mask image, I_{mask} from the binary image, BW will remove the frame as shown in Figure 11(c).

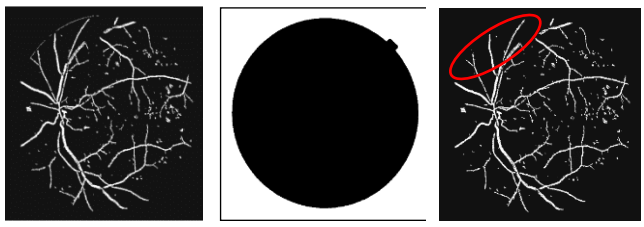

(a) (b) (c)

Figure 11: (a) Binary image with the frame (b) Mask image (c) Binary image of removal frame indicated in the red circle

The masked image, I_{mask} was performed using Otsu global thresholding technique. This technique turns the image into a binary image with the intensity of black (0) and white (1). In other to obtain a masked image, the threshold value should be selected within 0 and 1. This step helps to clear the frame of the retinal image. For further understanding, the mathematical equation of retinal frame removal was presented in Equation (11).

$$BW_1(x,y) = \begin{cases} 1 & if\ BW - I_{mask} > 0 \\ 0 & otherwise \end{cases} \quad (11)$$

2) Microaneurysms detection

Microaneurysms were detected by removal of retinal vessels and other dark lesions. The function *'bwareaopen'* was applied onto the binary image of size in between 10 to 20 pixels. The objects that have pixel size lower and greater than threshold value were eliminated from the image [18]. Thus, undesired foreground such as a retinal vessel, haemorrhages and noises were removed from the image and keeping only microaneurysms as shown in Figure 12.

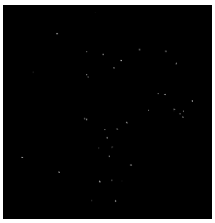

Figure 12: Binary image containing microaneurysms

III. Result and Discussion

As mention in the previous section, the main concern of the paper was to detect and graded the microaneurysms. The number of MAs counted will determine the severity of non-proliferative diabetic retinopathy (NPDR). NPDR was graded into normal, mild, moderate and severe based on the number of detected microaneurysms. The number of microaneurysms and its severity is presented in Table 1 [19].

Table 1
The Severity of NPDR [4]

	Grade	Classification
0	Normal	MA = 0
1	Mild	0 < MA ≤ 5
2	Moderate	5 < MA ≤ 15
3	Severe	MA > 15

MA = microaneurysms

Random MESSIDOR database of 40 images was analysed to grade the severity of the retinal disorder. From Table 2, it has been found that 24 images were detected as true grading which contributes 60%. Meanwhile, the other 40 % shows false grading of NPDR. Some of the previous research pay more concern on detection of MAs by evaluating the performance measures of microaneurysms such as sensitivity, specificity and accuracy rather than graded its severity [4,7].

Table 2
Percentage of Grade Detected by the Proposed Method

MESSIDOR database	True grading (TG)	False grading (FG)	Percentage grade [TG/(TG +FG) ×100]
40	24	16	60%

The main limitation of this study is due to misdetection of MAs and other dark lesions. Up to the removal of the retinal boundary, the MAs are still detected. However, after post processing whereby the MAs were extracted, some of them went missing. This issue will affect the grading of NPDR. Since the grading on NPDR unable to reach a higher percentage of detection, perhaps some segmentation techniques can be further extended by using feature extraction parameters such as circularity, colour, and area instead of pixel size [20].

IV. CONCLUSION

From the research that has been conducted, it is possible to conclude that the detection of MAs is important to confirm the severity of the retinal disorder. The proposed approach has demonstrated techniques such as filtration, background exclusion, contrast enhancement, h-maxima transform, multilevel thresholding and morphological closed operation. The percentage of severity grade that correctly detected when compared to ground truth grading is 60%. Based on the results, it shows that the findings are quite convincing. However, further research is required to improve the performance of the detection of MAs. In application, this research has great potential and ability to help the ophthalmologist in controlling the progression of DR.

ACKNOWLEDGEMENT

This research was supported by the Fundamental Research Grant Scheme (9003-00517) sponsored by Ministry of Higher Education Malaysia.

REFERENCES

[1] "World Diabetes," *A newsletter from World Health Organisation (WHO)*, p. 4, 1998.
[2] O. Faust, R. Acharya U., E. Y. K. Ng, K. H. Ng, and J. S. Suri, "Algorithms for the Automated Detection of Diabetic Retinopathy Using Digital Fundus Images: A review," *J. Med. Syst.*, vol. 36, no. 1, pp. 145–157, 2012.
[3] M. Usman Akram, S. Khalid, A. Tariq, S. A. Khan, and F. Azam, "Detection and Classification of Retinal Lesions for Grading of Diabetic Retinopathy," *Comput. Biol. Med.*, vol. 45, pp. 161–171, 2014.
[4] A. Sopharak, B. Uyyanonvara, and S. Barman, "Simple Hybrid Method for Fine Microaneurysm Detection from non-dilated Diabetic Retinopathy Retinal Images," *J. Comput. Med. Imaging Graph.*, vol. 37, pp. 394–402, 2013.
[5] "Diabetic Retinopathy-NPDR," *WillsEye Hospital*. [Online]. Available: https://www.willseye.org/video/diabetic-retinopathy-npdr.
[6] M. U. Raghu and P. Manohar, "A Simple Approach for the Detection of Microaneurysms Using Morphological Transform," *Int. J. Innov. Res. Comput. Commun. Eng.*, vol. 4, no. 7, pp. 13121–13123, 2016.
[7] K. Nemade and P. K. S. Bhagat, "Microaneurysms Detection from Retinal Image and Diabetic Retinopathy Grading," *Int. J. Emerg. Trends Technol. Comput. Sci.*, vol. 4, no. 4, pp. 74–77, 2015.
[8] A. Sopharak, B. Uyyanonvara, and S. Barman, "Automatic Microaneurysm Detection from Non-dilated Diabetic Retinopathy Retinal Images," *Proceeding World Congr. Eng.*, vol. 2, 2011.
[9] M. D. Saleh and C. Eswaran, "An efficient Algorithm for Retinal Blood Vessel Segmentation Using H-maxima Transform and Multilevel Thresholding," *Comput. Methods Biomech. Biomed. Engin.*, vol. 15, no. 5, pp. 517–525, 2012.
[10] S. SB and V. Singh, "Automatic Detection of Diabetic Retinopathy in Non-dilated RGB Retinal Fundus Images," *Int. J. Comput. Appl.*, vol. 47, no. 19, pp. 26–32, 2012.
[11] M. D. Saleh and C. Eswaran, "An Automated Decision-support system for Non-proliferative Diabetic Retinopathy Disease Based on MAs and HAs Detection," *Comput. Methods Programs Biomed.*, vol. 108, no. 1, pp. 186–196, 2012.
[12] "Methods to Evaluate Segmentation and Indexing Techniques in the Field of Retinal Ophthalmology (MESSIDOR)," *Advanced Concepts in Imaging Software (ADCIS)*, 2017. [Online]. Available: http://www.adcis.net/en/Download-Third-Party/Messidor.html. [Accessed: 23-May-2017].
[13] E. Decencière *et al.*, "Feedback on a Publicly Distributed Image Database: The Messidor Database," *Image Anal. Stereol.*, vol. 33, no. 3, pp. 231–234, 2014.
[14] M. Nagu and N. V. Shanker, "Image De-Noising By Using Median Filter and Weiner Filtering," *Int. J. Innov. Res. Comput. Commun. Eng.*, vol. 2, no. 9, pp. 5641–5649, 2014.
[15] M. Sridevi and C. Mala, "Multilevel Threshold Selection for Image Segmentation using Soft Computing Techniques," *Soft Comput.*, vol. 20, no. 5, pp. 1793–1810, 2016.
[16] S. Arora, J. Acharya, A. Verma, and P. K. Panigrahi, "Multilevel Thresholding for Image Segmentation Through a Fast Statistical Recursive Algorithm," *Pattern Recognit. Lett.*, vol. 29, no. 2, pp. 119–125, 2008.
[17] V. Y. Koli, A. G. Andurkar, and H. S. Jain, "Automatic Blood Vessel Segmentation in Retinal Image Based on Mathematical Morphology," *Int. J. Inven. Eng. Sci.*, vol. 2, no. 12, pp. 33–37, 2014.
[18] C. M Patil, "An Approach for the Detection of Vascular Abnormalities in Diabetic," *Int. J. Data Min. Tech. Appl.*, vol. 2, no. December, pp. 246–250, 2013.
[19] V. S. Hari, V. P. Jagathy Raj, and R. Gopikakumari, "Quadratic Filter for the Enhancement of Edges in Retinal Images for the Efficient Detection and Localization of Diabetic Retinopathy," *Pattern Anal. Appl.*, vol. 20, no. 1, pp. 145–165, 2017.
[20] C. Sundhar and D. Archana, "Automatic Screening of Fundus Images for Detection of Diabetic Retinopathy," *Int. J. Comput. Technol.*, vol. 2, no. 1, pp. 100–105, 2014.